



# Experimental Study on Mechanical Behavior of Unsaturated Silty Sand in Constant Equivalent Granular Void Ratio

Erfan Chali · Mohammad Maleki

Received: 24 November 2018 / Accepted: 14 August 2020 / Published online: 25 August 2020  
© Springer Nature Switzerland AG 2020

**Abstract** In this paper effect of fine mineralogy on mechanical behavior of unsaturated silty sand in different fine contents and divers confining pressure has been studied. All samples were molded with constant equivalent granular void ratio well-known parameter already proposed for characterizing silty sand behavior in saturated state. This manner of study allow to investigate also the validity of equivalent granular void ratio concept in unsaturated state. For this purpose, a series of triaxial tests were performed on the sand specimens with different percentages of silt in the undrained saturated (CU) and unsaturated (CW) conditions. The results showed that the material types and aggregate distribution of the fines have enormous effects on the silty sand behavior. In addition, the shear strength in the unsaturated specimens changed as a function of the initial applied matric suction. A fewer performance of equivalent intergranular void ratio in the case of unsaturated state in comparison of saturated states was observed.

**Keywords** Matric suction · Silty sand · Equivalent intergranular void ratio · Fine content

## 1 Introduction

Natural sands usually contain some fines contents. These fines can be either clay or silt. Effect of silt on mechanical behavior of sand has been discussed by a great number of authors in literature (e.g. Kuerbis et al. 1988; Koester 1994; Lade and Yamamuro 1997; Thevanayagam 1998; Polito 1999; Thevanayagam et al. 2002; Xenaki and Athanasopoulos 2003; Bouckovalas et al. 2003; Naeini and Baziar 2004; Yang et al. 2006; Rahman and Lo 2008; Rahman et al. 2012; Nguyen et al. 2015). These studies show that the fines has considerable effects on the sand behavior. So that at a given constant void ratio and confining pressure increase in non-plastic fine up to a certain fine content (known as threshold fine content) undrained shear strength of soil deceases. However, adding fines content beyond threshold value, an increase in undrained shear strength is observed.

Mitchell (1976) paid attention for the first time to the effect of the inactive fine role in transferring the forces applied on the sand structure. On this basis an index known as skeleton void ratio was used for characterizing sand containing low values of non-plastic fine by several authors (e.g. Kuerbis et al. 1988; Georgiannou et al. 1990; Pitman et al. 1994; Thevanayagam 1998). The skeleton void ratio has the following expression:

---

E. Chali · M. Maleki (✉)  
Department of Civil Engineering, Bu-Ali Sina University,  
Hamedan, Iran  
e-mail: maleki@basu.ac.ir

E. Chali  
e-mail: erfanchali11@gmail.com

$$e_g = \frac{e + f_c}{1 - f_c} \quad (1)$$

In which  $e$  is the soil void ratio and  $f_c$  is the fines content. For a given constant skeleton void ratio, an increase in  $f_c$  leads to decrease in void ratio ( $e$ ), so that for high value of fines content, mixture may be stronger than host sand. On the other word the effect of fines cannot be ignored. On this basis Thevanayagam (2000), introduced equivalent intergranular void ratio for ( $f_c < f_{cth}$ ) as:

$$(e_g)_{eq} = \frac{e + (1 - b)f_c}{1 - (1 - b)f_c} \quad (2)$$

In which  $f_c$  is the fines content and  $b$  is the part of the fines that actively participates in the intergranular contacts. This parameter is dependent on the soil grading and the amount of fines existing in the soil. Rahman and Lo (2008) proposed the following equation for calculating  $b$ :

$$b = \left[ 1 - \exp\left(-m \frac{(f_c/f_{cth})^n}{k}\right) \right] \cdot \left( r \frac{f_c}{f_{cth}} \right)^r \quad (3)$$

where  $f_c$  is the fines content,  $f_{cth}$  is the threshold fines content,  $r = \chi^{-1} = d_{50}/D_{10}$ , where subscripts denote fractile passing (10% for the sand-size fractile and 50% for the fines fractile),  $k = (1 - r)^{0.25}$  and  $m$  and  $n$  are the experimental constants. Rahman and Lo (2008) also proposed Eq. 4 for calculating the threshold fines content.

$$f_{cth} = A \left( \frac{1}{1 + e^{\alpha - \beta \chi}} + \frac{1}{\chi} \right) \quad (4)$$

In this relation,  $A$  is the dimensionless parameter  $\alpha$  and  $\beta$  are parameters related to the soil type.

Laboratory tests results at critical state in the  $e$ - $\log p'$  plane has been considered as a reference curve for describing shear resistance of sand (Been and Jefferies 1985; Konrad 1988; Ishihara 1993). In this regard contractancy and dilatancy states can be expressed by definition of certain state parameters characterized by distance between initial state and critical state curve at a given mean effective stress. In the case of silty sand, based on diverse experimental works (Bouckovalas et al. 2003; Naeini and Baziar 2004; Yang et al. 2006) the position of critical state line in the  $e$ - $\log p'$  coordinates changes depending on percentage of added silt. However, using equivalent

intergranular void ratio instead of void ratio the critical state lines converges so that a unique critical state curve can be deduced (Rahman and Lo 2007; Mohammadi and Qadimi 2015). Besides of shear resistance, dependence of small strain shear modulus of silty sand to density through equivalent void ratio was investigated by several authors (Goudarzy et al. 2016).

Several experimental studies have been performed on the silty sandy soils in unsaturated conditions (e.g. Wang et al. 2010; Maleki and Bayat 2012; Schnellmann et al. 2013; Zhou et al. 2016; Patil et al. 2017). These researches have shown that the factors such as loading path, density and matric suction affect the mechanical behavior of silty sand in unsaturated state. However, there is not much of the information in the literature regarding the effect of the silt material types on the behavior of these soils in the unsaturated conditions and particularly the performance of the silty sand equivalent intergranular void ratio relations in the unsaturated conditions.

In this research, the factors affecting the sandy soil behavior with two types of natural and rock powder silts with different percentages of the fines in the saturated and unsaturated conditions were studied. In order to examine the performance of  $(e_g)_{eq}$  in estimating the silty sand resistance, all the specimens were molded with an identical  $(e_g)_{eq}$ . Some saturated (CU) and unsaturated (CW) triaxial tests were conducted for this purpose.

## 2 Test Program

### 2.1 Testing Apparatus

The utilized unsaturated triaxial apparatus is capable of using the axis translation technique. The total volume variation and the pore water pressure are independently measured during the test by the use of the double cells system. The air entry value used for the ceramic disks in this research is 500 kPa. Figure 1 shows detailed images of triaxial double cells and its base plate.

### 2.2 Materials

The soil used in this research is silty sand. In order to assess the effect of the fines material types on the soil

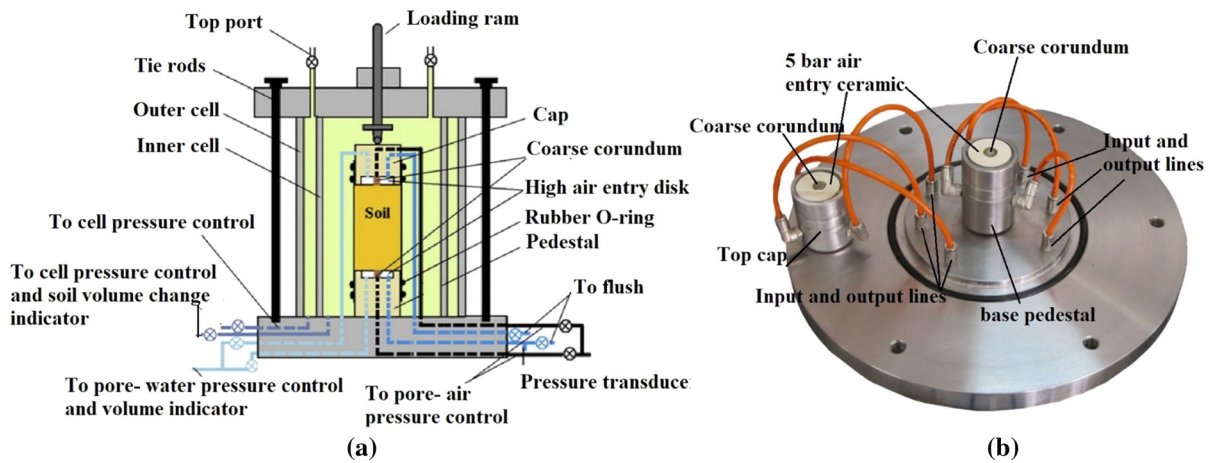


**Fig. 1** Details of triaxial cells (a) and cells base plate (b) (Maleki and Bayat 2012)

behavior, two silt types of natural and rock powder are used which are named as silt1 and silt2, respectively. Particle size distribution of clean sand and two types of silts are presented in the Fig. 2 which are obtained based on ASTM D422. Some characteristics of sand-silt mixtures, calculated from particle distribution curves, are presented in the Table 1.

Atterberg limits tests, based on ASTM D-4318 were carried out. The obtained results showed that two types of used silts are in non-plastic state. Specific gravity of clean sand, silt1 and silt2 by performing related tests based on ASTM D-854 were, 2.65, 2.7 and 2.68 respectively. Images of natural silt (silt1) and rock powder (silt2) are presented in Fig. 3.

In order to find the constituents of the silts and the particles shapes, the XRD test (Fig. 4) and microscope imaging (Fig. 5) were used, respectively. The XRD test results revealed that the silt2 is made from Quartz

mineral; but silt1 contains clayey minerals including Illite and Kaolinite in addition to the non-clayey minerals of Quartz, Feldspar and Mica. The imaging by microscope also showed that the silt1 particles are mostly rounded while the most part of silt2 particles are angular (Fig. 5).

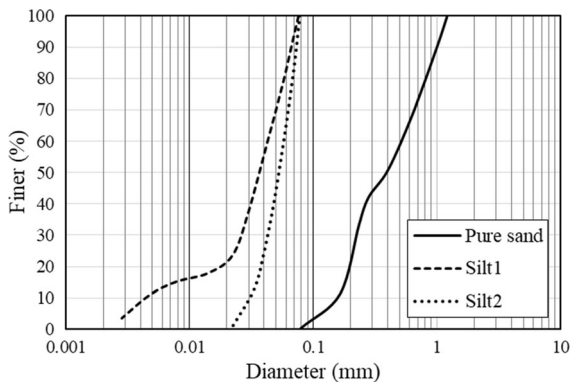
### 2.3 Sample Preparation

The equivalent intergranular void ratio in saturated and unsaturated tests are considered to be 0.85 in the present research. The global void ratio values of all the specimens are obtained as presented in Table 2 by the use of Eq. 2. The percentages of the threshold fines for the silt1 and silt2 are obtained 29.68 and 31.55, respectively, by using Eq. 4.

### 2.4 Experimental Detail

#### 2.4.1 Saturated State

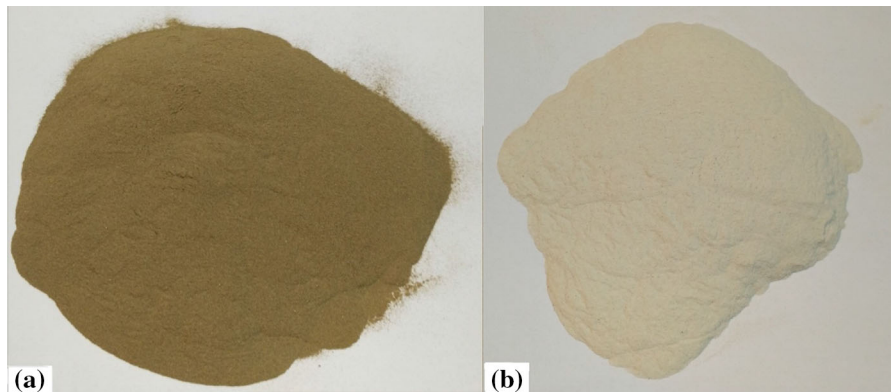
Various researchers concluded during their examination that the specimen construction method affects the results of the triaxial tests (Mulilis et al. 1977; Kuerbis and Vaid 1988). The specimens are molded by the wet tamping method in 6 layers in this research. After molding the specimens, the carbon dioxide gas (CO<sub>2</sub>) was inserted for at least 2 h to facilitate saturation process of the specimens. After inserting the carbon dioxide gas, the de-aired water was passed through the specimen. After this step, the back pressure was applied on the specimen. The parameter of the



**Fig. 2** Grain size distribution curve

**Table 1** Characteristics of soils

Fine content (%)	Silt type	D <sub>10</sub>	D <sub>30</sub>	D <sub>50</sub>	D <sub>60</sub>	C <sub>u</sub>	C <sub>c</sub>
10	Silt1	0.075	0.197	0.311	0.448	5.97	1.15
15	Silt1	0.045	0.182	0.281	0.411	9.13	1.79
20	Silt1	0.037	0.173	0.255	0.371	10.02	2.18
10	Silt2	0.075	0.197	0.311	0.448	5.97	1.15
15	Silt2	0.062	0.182	0.280	0.411	6.63	1.30
20	Silt2	0.053	0.173	0.254	0.377	7.11	1.50

**Fig. 3** Images of silts used **a** natural silt (silt1), **b** rock powder (silt2)

Skempton pore water pressure was used to control the specimen saturation degree. Based on the ASTM D 4767 one can consider a soil to be saturated when the Skempton coefficient is higher than 95%. The specimens were consolidated under three confining pressures of 100, 150 and 200 kPa at the end of the saturation step. Then, they were sheared with a constant loading rate. The loading rate was considered to be 0.5 mm per minute according to the soil type.

#### 2.4.2 Unsaturated State

Similar to the saturated specimens, the wet tamping method is used in this case for molding the specimens. Since the wetting or drying path affects the behavior of the unsaturated soils (Han et al. 1995; Nishimura and Fredlund 2002; Rahardjo et al. 2004; Guan et al. 2009; Chiu et al. 2014); the moisture content for molding the specimens is considered in a way that the specimens stay in the drying path. The specimens were placed on the previously saturated ceramic disks after being molded. After applying the initial suction and the

consolidation stress, the specimens were loaded with the velocity of 0.04 mm/min. An image of deformed specimen at the failure state is displayed in “Appendix”. The specimens were named in a way that presents their test conditions. For example, Silt1, f10, S100, c50 represents a test which uses silt1. The fines content is also 10%, the suction is 100 kPa and the confining pressure is 50 kPa. The initial values of matric suction and net stress for different specimens are presented in Table 3.

### 3 Results and Discussions

Results of the tests were drawn in the  $q$ - $\varepsilon_a$  coordinates. Deviator stress of  $q$  is the difference between major and minor principal stresses;  $\sigma_1$  and  $\sigma_3$ .  $\varepsilon_a$  represents axial strain applied on the specimens. For comparing the results, this paper focuses on the maximum and ultimate (critical) deviator stresses denoted as  $q_{max}$  and  $q_{critical}$ , picked up from the curves of  $q$ - $\varepsilon_a$ . However, some  $q$ - $\varepsilon_a$  curves are presented in the “Appendix”.

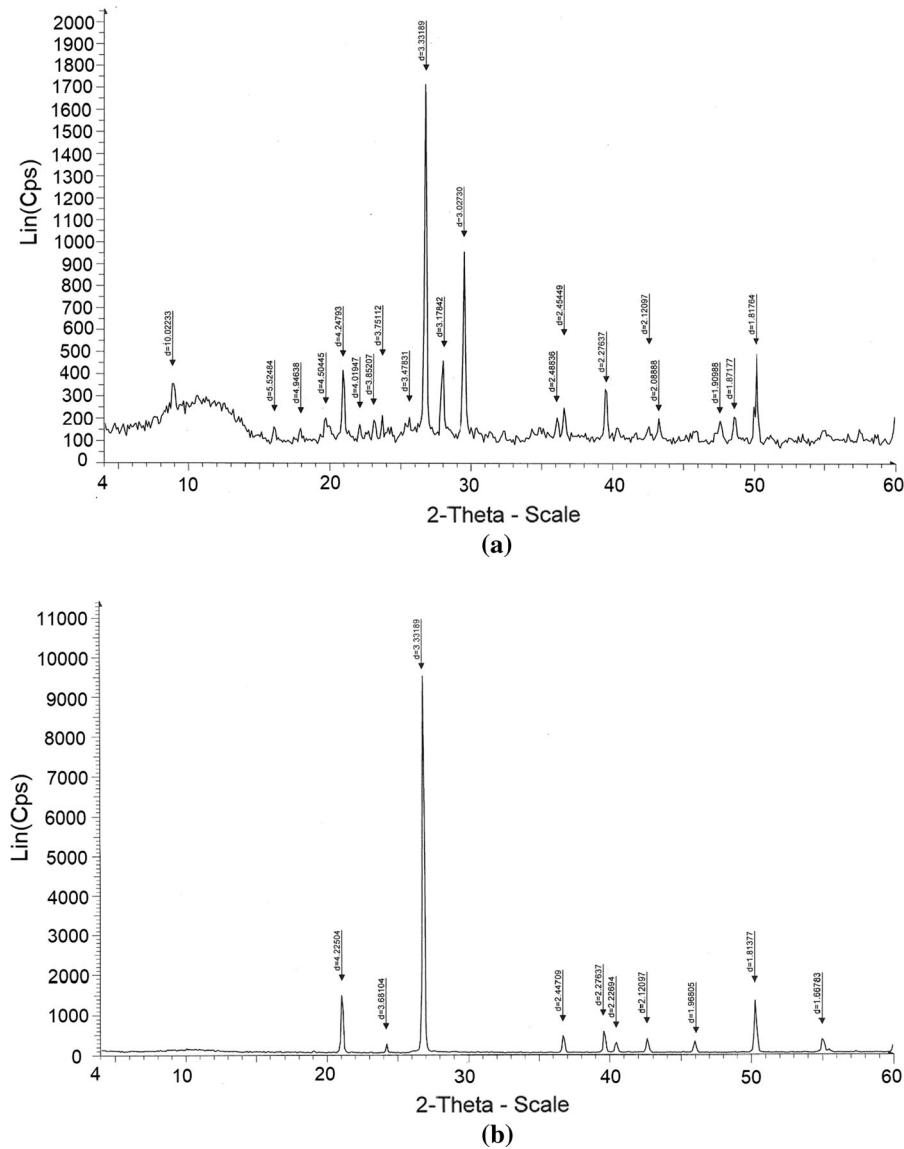


**Fig. 4** XRD test result **a** silt1, **b** silt2

### 3.1 Saturated State

#### 3.1.1 Effect of Different Factors on Deviator Stress at Peak State

The diagram of the maximum deviator stress versus the confining pressure is shown in Fig. 6. As it was expected, the  $q_{max}$  increased by the increase of the confining pressure. By increasing the confining pressure from 100 kPa to 150 kPa, the maximum deviator stresses were increased by 31 and 42% in specimens

having silt1 and silt2, respectively. Changing the confining pressure from 150 kPa to 200 kPa has led a reduction in the  $q_{max}$  increase rate; so that the average increase rate in both silt types is 21% in this case.

As it can be seen, there is no considerable change in the maximum deviator stress when the fines content is increased in the specimens having silt1; but the maximum deviator stress is increased in specimens having silt2. The increase rate of the  $q_{max}$  in this silt is dependent on the fines content. This rate reduces by increasing the fines content.

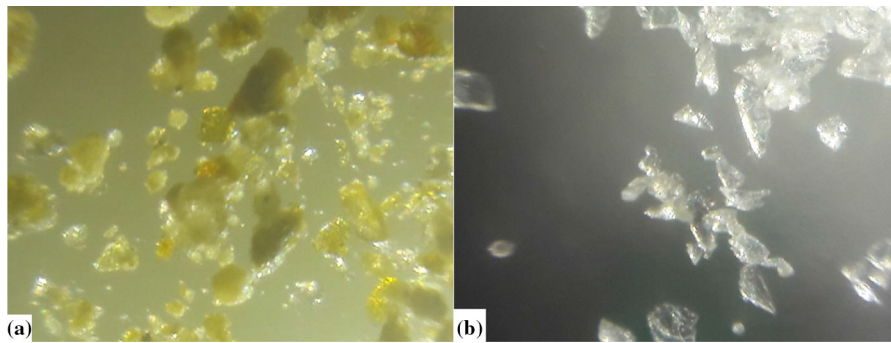


**Fig. 5** Microscopic image of the silts used **a** silt1, **b** silt2

**Table 2** Global void ratio of saturated and unsaturated samples

Fine content (%)	Silt type	$e_{total}$
10	Silt1	0.694
15	Silt1	0.638
20	Silt1	0.595
10	Silt2	0.693
15	Silt2	0.638
20	Silt2	0.598

Another important point which can be found from the diagrams of Fig. 6 is that the fine material types in specimens with 10% silts does not have considerable

**Table 3** Initial matric suction and net stress values for the constant water content tests

Test	Fine content (%)	$u_a - u_w$ (kPa)	$\sigma_3 - u_a$ (kPa)
(Silt1 or Silt2), f10, S100, c50	10	100	50
(Silt1 or Silt2), f10, S100, c100	10	100	100
(Silt1 or Silt2), f10, S100, c150	10	100	150
(Silt1 or Silt2), f10, S150, c100	10	150	100
(Silt1 or Silt2), f10, S200, c150	10	200	100
(Silt1 or Silt2), f15, S100, c50	15	100	50
(Silt1 or Silt2), f15, S100, c100	15	100	100
(Silt1 or Silt2), f15, S100, c150	15	100	150
(Silt1 or Silt2), f15, S150, c100	15	150	100
(Silt1 or Silt2), f15, S200, c150	15	200	100
(Silt1 or Silt2), f20, S100, c50	20	100	50
(Silt1 or Silt2), f20, S100, c100	20	100	100
(Silt1 or Silt2), f20, S100, c150	20	100	150
(Silt1 or Silt2), f20, S150, c100	20	150	100
(Silt1 or Silt2), f20, S200, c150	20	200	100

effect on the results. For instance, for the fines content of 10% and the confining pressure of 100 kPa, the maximum deviator stresses for the sand with silt1 and silt2 are obtained 72 kPa and 71 kPa, respectively. The difference between the results of the two fines material types increases by increasing the silt percentage from 10 to 15.

### 3.1.2 Effect of Different Factors on Deviator Stress at Critical State

The diagrams of the ultimate deviator stress versus the confining pressure for different percentages of the silt are shown in Fig. 7. Similar to the previous case, the  $q_{critical}$  is increased by the increase of the confining pressure. The average increase rates of the ultimate

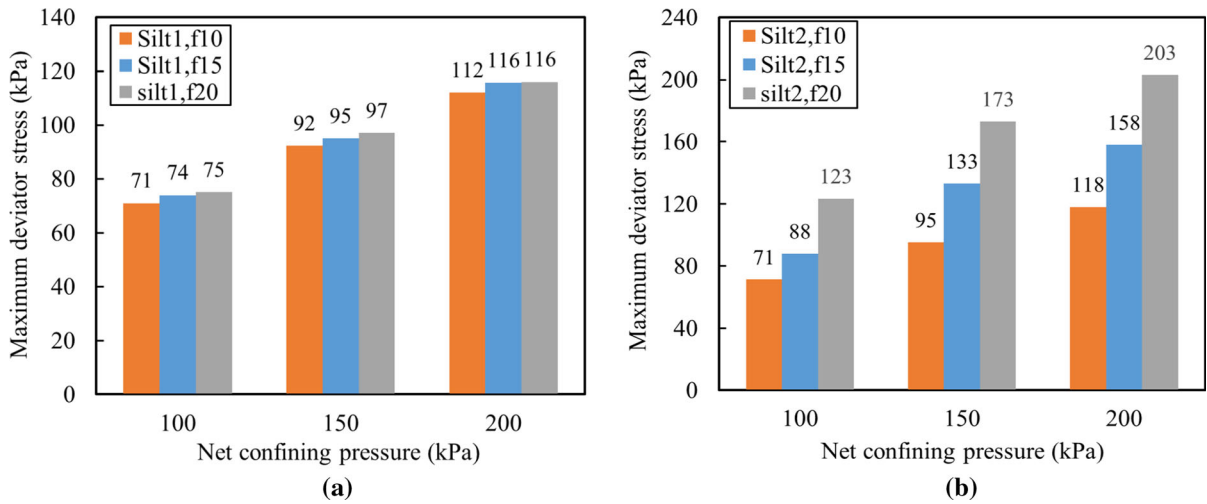


**Fig. 6** The influence of confining pressure on maximum deviator stress **a** silt1, **b** silt2

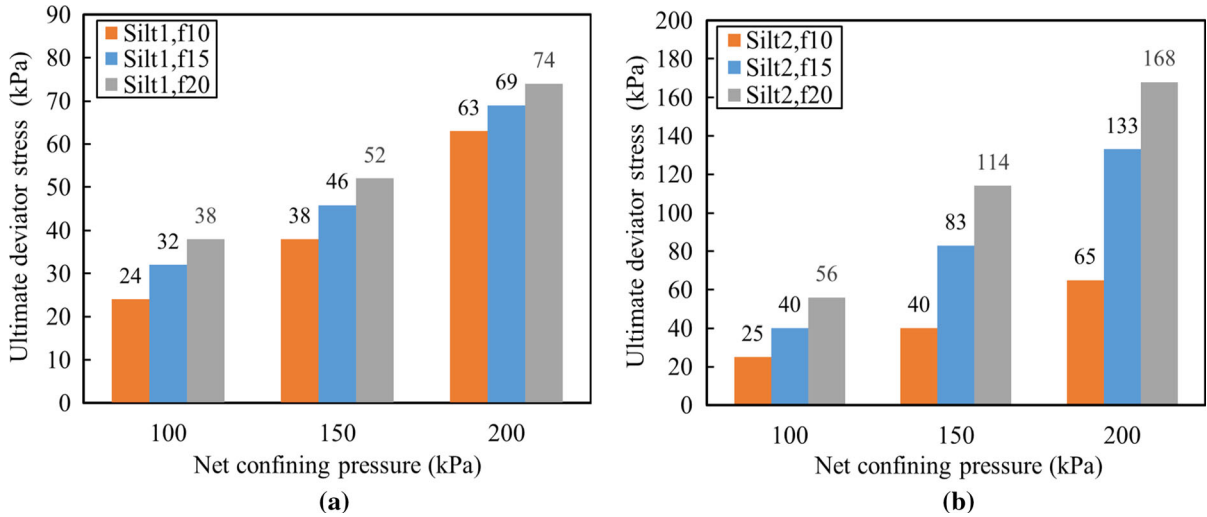


**Fig. 7** The influence of confining pressure on ultimate deviator stress **a** silt1, **b** silt2

and the maximum deviator stresses are presented in Table 4 for better comparison. As it can be seen, the increase of the confining pressure has more effects on the  $q_{critical}$ .

Also for the fines content 10% and the identical confining pressures in this case, the ultimate deviator stresses of the both silt types are almost equal with each other. The main difference visible in the results of

**Table 4** The effect of increasing the confining pressure on the maximum and ultimate deviator stress rate

Fine type	Increasing the confining pressure (kPa)	Increase rate of $q_{max}$ (%)	Increase rate of $q_{critical}$ (%)
Silt1	100–150	31	46
	150–200	21	53
Silt2	100–150	42	90
	150–200	21	57

this section is that the ultimate deviator stress increases in the specimens having silt1 by the increase of the fines content; while the maximum deviator stresses in these specimens had no significant change, for the identical confining pressures, by the increase of the fines content.

### 3.1.3 Effect of Different Factors on Pore Water Pressure

The diagrams of the pore water pressure versus the confining pressure show that the results of the two silt types are almost identical for 10% of the fines (Fig. 8). One can observe a slight decrease in the pore water pressure by increasing the fines content in specimens having fines of silt type 1; but the pore water pressure experienced a significant decrease by increasing the fines content in the specimens containing silt2. It should be noted that this increase is higher in specimens experiencing the fines content increase from 10 to 15% compared to those experiencing the fines content increase from 15 to 20%.

As it has been mentioned, all specimens were molded in the state of constant intergranular void ratio, so, it was expected the same behaviors for a given confining pressure. However, maximum and ultimate deviator stresses and pore water pressure were different, depending on the fine percentage and type.

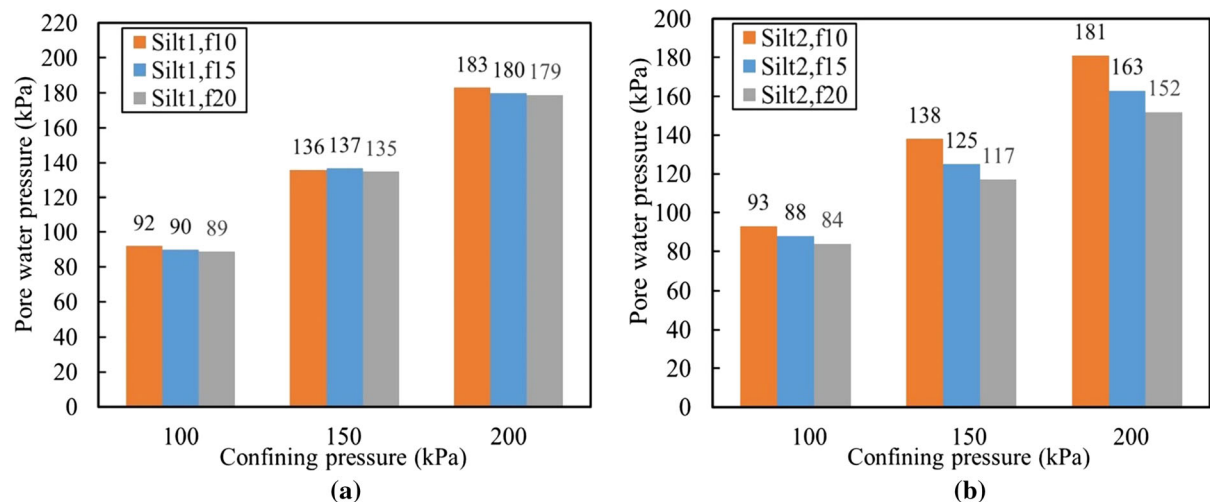


**Fig. 8** The influence of confining pressure on pore water pressure **a** silt1, **b** silt2

## 3.2 Unsaturated State

The results of the unsaturated triaxial tests (CW) are presented in this section in the two categories of the constant confining pressure (100 kPa) and the constant suction (100 kPa).

### 3.2.1 Constant Confining Pressure (100 kPa)

The diagrams of the maximum deviator stress versus the initial suction for constant confining pressure of 100 kPa are illustrated in Fig. 9a, b for the comparison of the effect of the initial suction on the specimen maximum strength. As it can be seen, the  $q_{max}$  in the specimens containing 10% silt linearly increases by increasing the initial suction; but was seen a change in the soil behavior by increasing the silt percentage from 10 to 15 and 20%. No significant variation can be observed in  $q_{max}$  values in all the specimens by increasing the initial suction from 150 to 200 kPa; while increasing the initial suction from 100 to 150 kPa has led to an increase in the maximum deviator stress. The magnitude of this increase depends on the silt material types and percentage which will be discussed.

- This increase is 8% in specimens containing 15% of silt1. This value reduces to 3.5% by increasing the silt percentage from 15 to 20%.
- This increase is 5% in specimens containing 15% of silt2. There is no significant increase in this



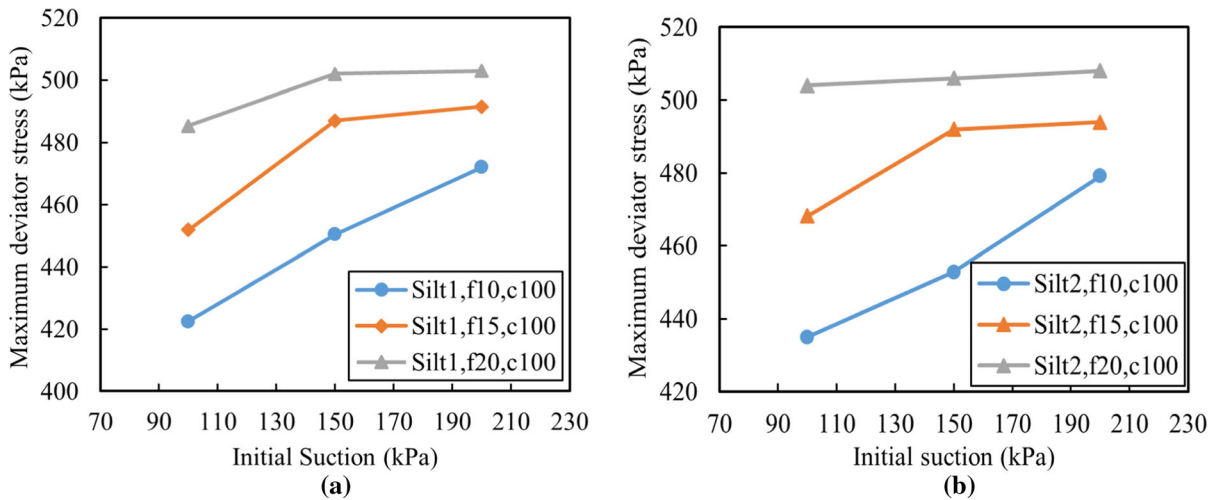


**Fig. 9** Maximum deviator stress versus initial suction **a** silt1, **b** silt2

value when the silt percentage is raised from 15 to 20%.

By examining the obtained results one can observe that there is a fall after the maximum strength in some specimens. Thus, the diagram of the ultimate deviator stress versus the initial suction is illustrated in Fig. 10. Similar to Fig. 9, increasing the initial suction has led to a linear increase in the  $q_{critical}$  of the specimens containing 10% of silt. This behavior is observed in both silt types. However, increasing the fines content causes the specimens behavior to change. The ultimate deviator stress variation in specimens having silt1 is similar to the maximum deviator stress; but the

behavior is different in specimens having silt2.  $q_{critical}$  in these specimens for the percentages of 15 and 20 is reduced.

The experiments results also reveal that there is an increase in the strength by increasing the silt percentage. This strength increase is caused by the specimen density increase due to the fines content rise.

### 3.2.2 Constant Suction (100 kPa)

Since no strain softening was observed after the maximum deviator stress of the specimens in this category the variation of the  $q_{max}$  is, therefore, presented in this section. The diagram of the

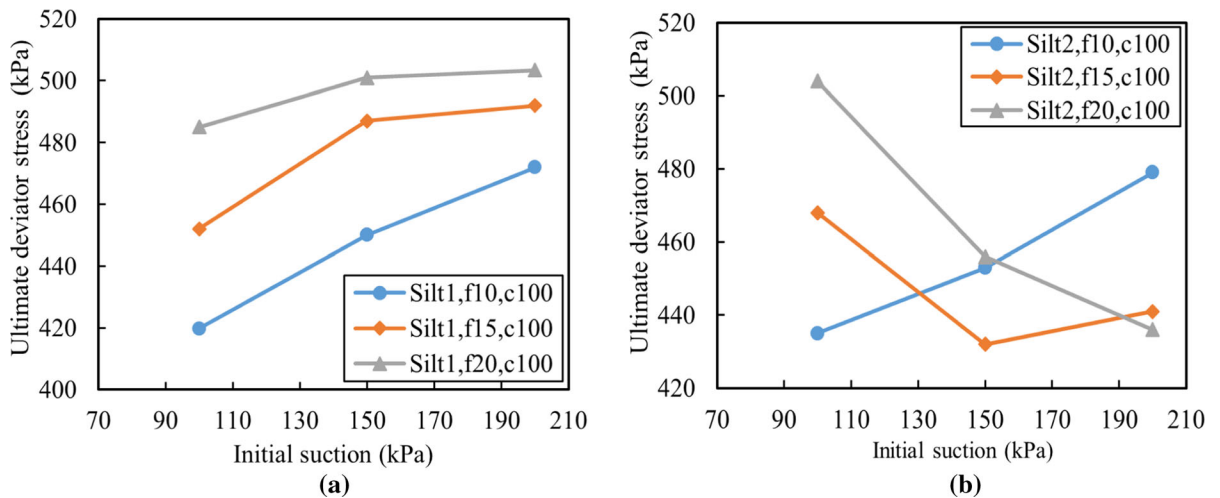


**Fig. 10** Ultimate deviator stress versus confining pressure **a** silt1, **b** silt2

maximum deviator stress versus the confining pressure is illustrated in Fig. 11. The increase rates of the maximum deviator stresses for different percentages of the fines are presented in Table 5. The obtained results show that this increase depends on the fines material types, fines content and the confining pressure. The increase rate of the  $q_{max}$  decreases in all the specimens by increasing the confining pressure. Moreover, in most cases, the increase rate of the maximum deviator stress is higher in specimens containing silt1. Increasing the fines content has also reduced this rate in most cases. As the final point, one can say that the effect of the confining pressure increase on the shear strength increase is by far higher than that of the suction increase. For instance, the soil  $q_{max}$  increases approximately by 46% when the confining pressure in the specimens containing 10% of silt (sit1) is increased from 100 to 150 kPa; but increasing the suction from 100 to 150 kPa, increases the  $q_{max}$  by just 8%. This result is in agreement with the results of the research of Pereira et al. (2006) and Maleki and Bayat (2012).

Similar to the saturated state, also this case, even though,  $(e_g)_{eq}$  was constant but, different behaviors were observed for a given confining pressure.

### 3.3 Critical State Line (CSL)

The critical state line represents a state which the soil has reached after the complete application of the shear. The unlimited plastic strains happen in the critical

state by the stress remaining constant. In this state, the rate of the pore water pressure production in the undrained tests and the volume variation production rate in the drained tests become zero. The critical state concepts are expressed in the three spaces of  $e:\log p'$ ,  $v:\ln p'$  and  $q:p'$ . The critical state line (CSL) in this research is examined in the  $q:p'$  plan in the two states of saturated and unsaturated.

#### 3.3.1 Saturated State

The critical state line in the  $q:p'$  space is as Eq. 5 (Schofield and Wroth 1968).

$$q = Mp' \quad (5)$$

The critical state line equations for different percentages of the fines content are shown in Fig. 12 based on the calculated different values of the ultimate deviator stress and the mean effective stress. The mean effective stress is calculated by Eq. 6.

$$p' = \frac{\sigma_1 + 2\sigma_3}{3} - u_w \quad (6)$$

The results show that using the same intergranular void ratio in molding the specimens has caused the critical state lines in the  $q:p'$  plan become nearly identical for different percentages of the fines. The silt particles materials have also no effect on this slope.

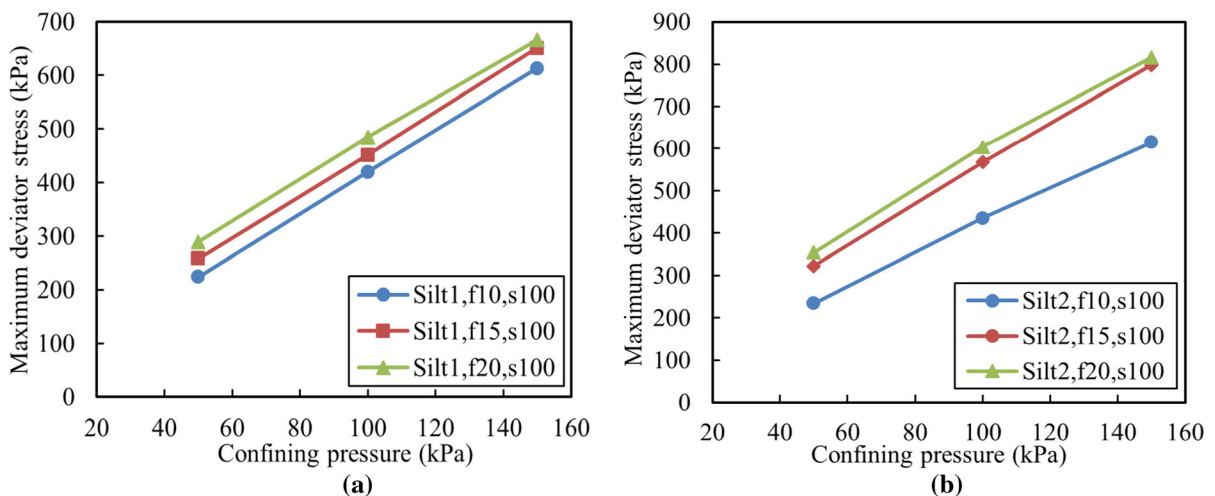


**Fig. 11** Maximum deviator stress versus confining pressure **a** silt1, **b** silt2

**Table 5** Maximum stress increase rate

Fine type	Increasing the fine content (%)	Confining pressure (kPa)	Maximum stress increase rate (%)
Silt1	From 10 to 15	50	15.6
		100	6.9
		150	6.2
	From 15 to 20	50	12.0
		100	8.2
		150	2.4
Silt2	From 10 to 15	50	15.3
		100	7.4
		150	4.8
	From 15 to 20	50	10.9
		100	7.6
		150	2.7

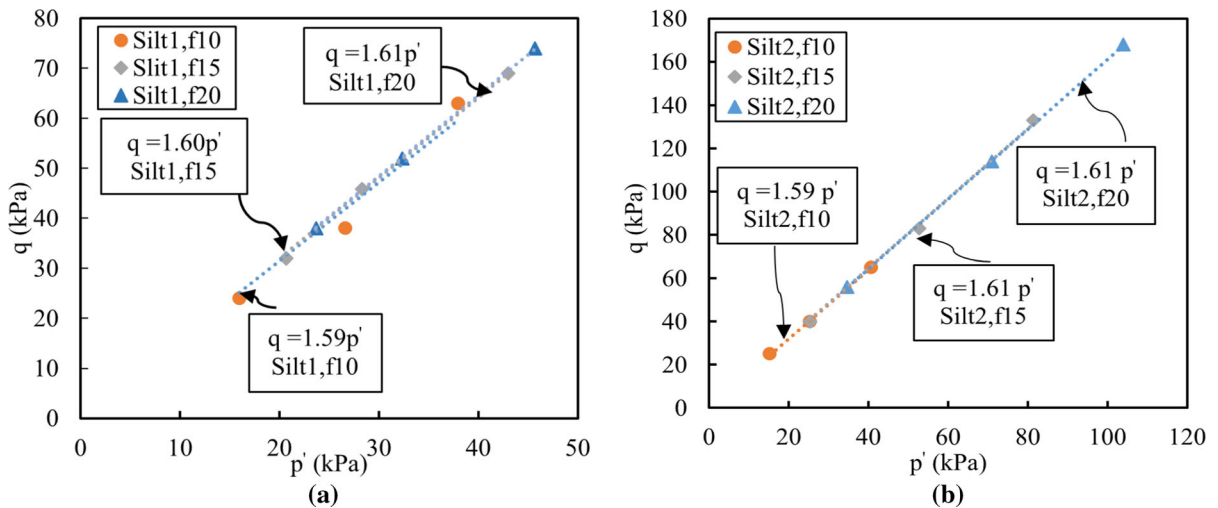


**Fig. 12** Critical state values for saturated test in  $q - p'$  coordinate **a** silt1, **b** silt2

3.3.2 Unsaturated State

Several studies have been performed in recent years for expressing the critical state in the unsaturated soils. These studies have led to a framework for the critical state concepts in the unsaturated soils (Alonso et al. 1990; Toll 1990; Wheeler and Sivakumar 1995; Loret and Khalili 2002; Wang et al. 2002; Toll and Ong 2003; Khalili et al. 2004).

In this research, the critical state line is plotted using the Bishop’s effective stress principle and the formulations proposed by Aitchison (1985) and

Khalili and Khabbaz (1998) for calculating the effective stress parameter for the suction of 100 kPa.

Bishop (1959):

$$\sigma' = (\sigma - u_a) + \chi(u_a - u_w) \tag{7}$$

Aitchison (1985):

$$\chi = \begin{cases} 1 & \text{if } S_r = 1 \\ \left( \frac{\alpha}{(u_a - u_w)_b} \right) (u_a - u_w)_b & \text{if } S_r < 1 \end{cases} \tag{8}$$

Khalili and Khabbaz (1998):

**Table 6** Air entry suction

Test	Air entry value (kPa)	Test	Air entry value (kPa)
Silt1, f10	10	Silt2, f10	12
Silt1, f15	13	Silt2, f15	16
Silt1, f20	15	Silt2, f20	20

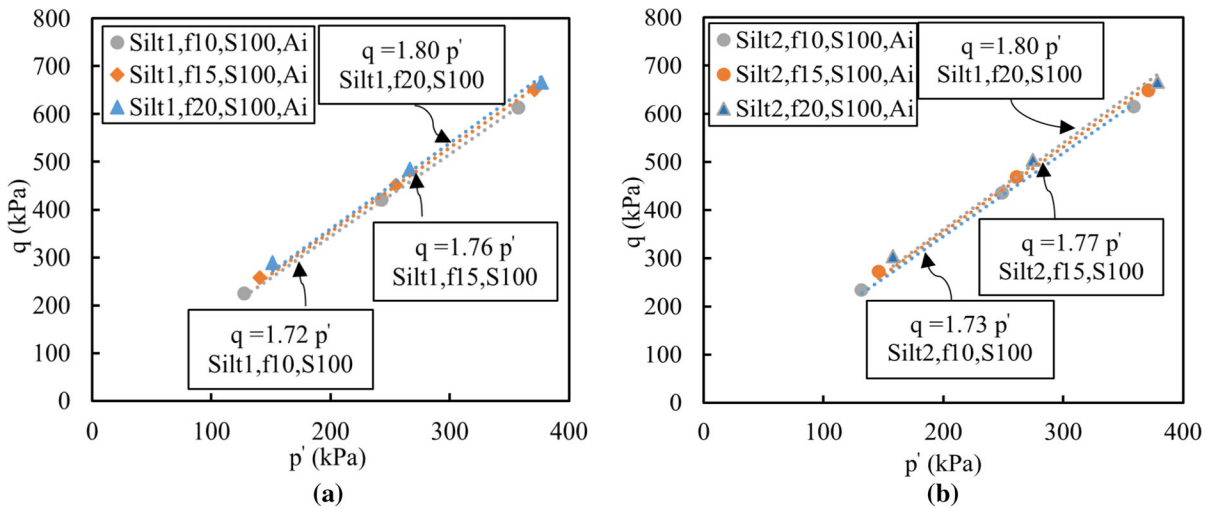


**Fig. 13** Critical state lines for unsaturated tests in  $q - p'$  coordinate (Aitchison (1985) effective stress parameter) **a** silt1, **b** silt2

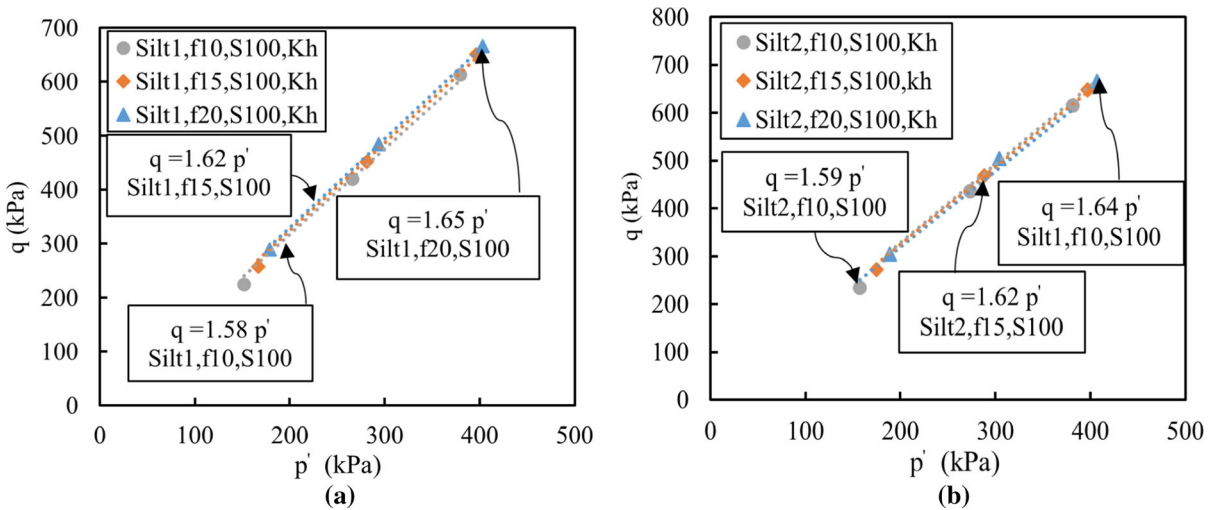
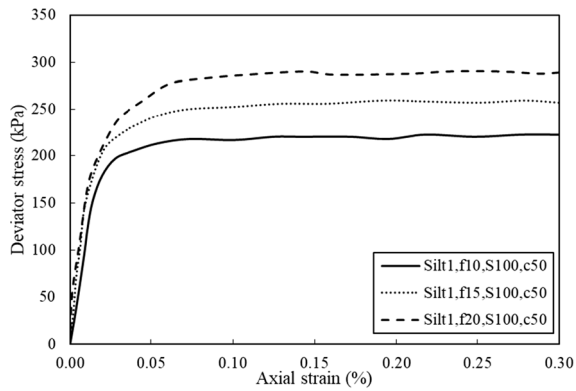


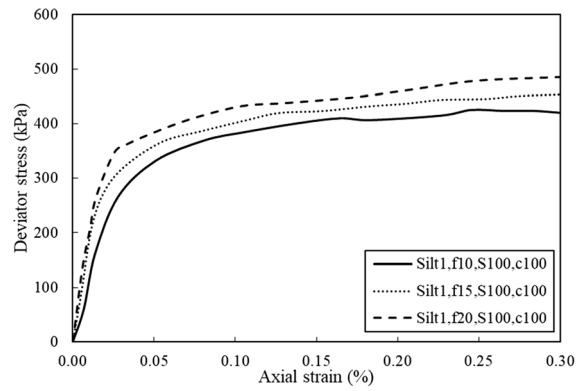
**Fig. 14** Critical state lines for unsaturated tests in  $q - p'$  coordinate (Khalili and Khabbaz (1998) effective stress parameter) **a** silt1, **b** silt2

$$\chi = \begin{cases} \left[ \frac{(u_a - u_w)}{(u_a - u_w)_b} \right]^{-0.55} & \text{if } (u_a - u_w) > (u_a - u_w)_b \\ 1 & \text{if } (u_a - u_w) \leq (u_a - u_w)_b \end{cases} \quad (9)$$

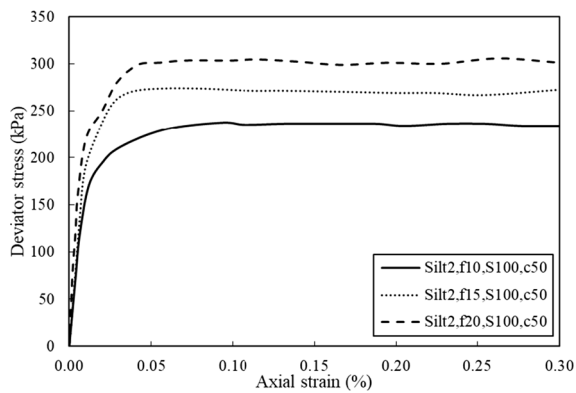
where  $(\sigma - u_a)$  is the net normal stress,  $(u_a - u_w)$  is the matric suction,  $(u_a - u_w)_b$  is the air entry suction,  $\alpha$  is a coefficient varying between 0.3 and 0.35 and  $S_r$  is



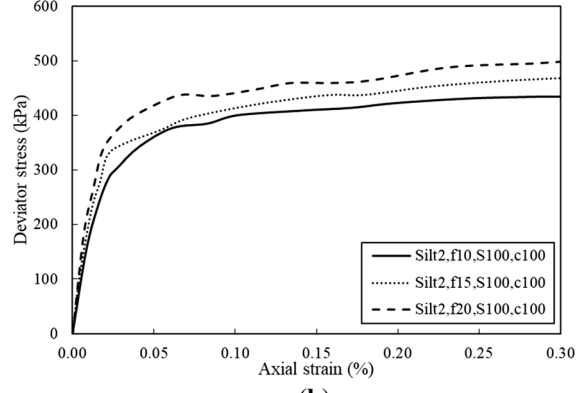
(a)



(a)



(b)



(b)

**Fig. 15** Stress–strain curves in unsaturated conditions with confining pressure of 50 kPa and initial suction of 100 kPa **a** Silt1, **b** Silt2

**Fig. 16** Stress–strain curves in unsaturated conditions with confining pressure of 50 kPa and initial suction of 100 kPa **a** Silt1, **b** Silt2

the moisture content. The values obtained for the air entries in different specimens are presented in Table 6.

Figure 13 shows the critical state line plotted using the Aitchison (1985) effective stress parameter. The achieved equations reveal that the slopes of the critical state lines are very different in the saturated and unsaturated states. By increasing the fines content, the slope is also increased. However, the slopes of the two critical state lines with different silt material types are similar when the fines content are identical; thus the fines material types and shape have no effect on the slope of the critical state line.

The critical state line is plotted in Fig. 14 using the Khalili and Khabbaz (1998) effective stress equation. Unlike the previous case, the obtained lines equations are nearly similar to that of the saturated state. The slope difference in the saturated and unsaturated states becomes larger by increasing the fines content. In this case, the slopes of the two critical state lines with

different silt material types and same fine content are identical. Ng et al. (2016) have previously reached this result in which the particles shape has no effect on the critical state line slope in the saturated state.

#### 4 Summary and Conclusions

- In low value of fine (10%), maximum and ultimate deviator stresses and corresponding pore water pressure for two types of fine were the same. However in the case of unsaturated state for the samples including 10% fine, maximum deviator stress was increased linearly as a function of initial matric suction.
- The results revealed that using the identical intergranular void ratio in molding the specimens causes the critical state lines slopes in the saturated



**Fig. 17** Failed unsaturated test specimen

space become similar for different fines content for the two silt types in the  $q:p'$  plan; however, it was observed that the variations of the maximum deviator stress, ultimate deviator stress and the pore water pressure are functions of the fines material type and percentage.

- Using the same intergranular void ratio in molding the specimens in the unsaturated state has led the critical state lines slopes to approximately converge to each other; of course, this convergence is lower in comparison with the saturated state. The reason behind it is the presence of the matric suction.

### Appendix: Deviatoric Stress Versus Axial Strain of Some Tests

As mentioned in the main text, this study aimed to investigate the factor affecting shear strength of unsaturated silty sand at given equivalent intergranular void ratio. However, some deviatoric stress-axial strain curves are presented in Figs. 15 and 16 which reveal nonlinear behaviour of unsaturated silty sand at the low levels of strain is also affected by different

factors particularly matric suction, fine type and percentage.

Also an image of deformed specimen at the failure state is displayed in Fig. 17.

### References

- Aitchison G (1985) Relationships of moisture stress and effective stress functions in unsaturated soils. In: Golden Jubilee of the International Society for Soil Mechanics and Foundation Engineering, Butterworth, London, pp 20–25
- Alonso EE, Gens A, Josa A (1990) Constitutive model for partially saturated soils. *Géotechnique* 40:405–430. <https://doi.org/10.1680/geot.1990.40.3.405>
- ASTM. Annual Book of ASTM Standards. American Society for Testing and Materials, West Conshohocken, United States
- Been K, Jefferies MG (1985) A state parameter for sands. *Géotechnique* 35:99–112. <https://doi.org/10.1680/geot.1985.35.2.99>
- Bishop A (1959) The effective stress principle. *Teknisk Ukeblad* 39:859–863
- Bouckovalas GD, Andrianopoulos KI, Papadimitriou AG (2003) A critical state interpretation for the cyclic liquefaction resistance of silty sands. *Soil Dyn Earthq Eng* 23:115–125. [https://doi.org/10.1016/S0267-7261\(02\)00156-2](https://doi.org/10.1016/S0267-7261(02)00156-2)
- Chiu CF, Ni XW, Zhang LS (2014) Effect of hydraulic hysteresis on shear strength of unsaturated clay and its prediction using a water retention surface. *Eng Geol* 173:66–73. <https://doi.org/10.1016/j.enggeo.2014.02.008>
- Georgiannou V, Burland J, Hight D (1990) The undrained behaviour of clayey sands in triaxial compression and extension. *Géotechnique* 40:431–449. <https://doi.org/10.1680/geot.1990.40.3.431>
- Goudarzy M, Rahman MM, König D, Schanz T (2016) Influence of non-plastic fines content on maximum shear modulus of granular materials. *Soils Found* 56:973–983. <https://doi.org/10.1016/j.sandf.2016.11.003>
- Guan GS, Rahardjo H, Choon LE (2009) Shear strength equations for unsaturated soil under drying and wetting. *J Geotech Geoenviron Eng* 136:594–606. [https://doi.org/10.1061/\(ASCE\)GT.1943-5606.0000261](https://doi.org/10.1061/(ASCE)GT.1943-5606.0000261)
- Han K, Rahardjo H, Broms B (1995) Effect of hysteresis on the shear strength of a residual soil. In: Proceedings of the 1st international conference on unsaturated soils. Paris, France, pp 499–504
- Ishihara K (1993) Liquefaction and flow failure during earthquakes. *Géotechnique* 43:351–451. <https://doi.org/10.1680/geot.1993.43.3.351>
- Khalili N, Khabbaz MH (1998) A unique relationship for  $\chi$  for the determination of the shear strength of unsaturated soils. *Géotechnique* 48:681–687. <https://doi.org/10.1680/geot.1998.48.5.681>
- Khalili N, Geiser F, Blight G (2004) Effective stress in unsaturated soils: review with new evidence. *Int J Geomech*

- 4:115–126. [https://doi.org/10.1061/\(ASCE\)1532-3641\(2004\)4:2\(115\)](https://doi.org/10.1061/(ASCE)1532-3641(2004)4:2(115))
- Koester JP (1994) The influence of fine type and content on cyclic strength. In: Ground failures under seismic conditions. ASCE, pp 330–345
- Konrad JM (1988) Interpretation of flat plate dilatometer tests in sands in terms of the state parameter. *Géotechnique* 38:263–277. <https://doi.org/10.1680/geot.1988.38.2.263>
- Kuerbis R, Vaid YP (1988) Sand sample preparation-the slurry deposition method. *Soils Found* 28:107–118. [https://doi.org/10.3208/sandf1972.28.4\\_107](https://doi.org/10.3208/sandf1972.28.4_107)
- Kuerbis R, Negussey D, Vaid YP (1988) Effect of gradation and fines content on the undrained response of sand. *Geotech Spec Publ* 21:330–345
- Lade PV, Yamamuro JA (1997) Effects of nonplastic fines on static liquefaction of sands. *Can Geotech J* 34:918–928
- Loret B, Khalili N (2002) An effective stress elastic–plastic model for unsaturated porous media. *Mech Mater* 34:97–116. [https://doi.org/10.1016/S0167-6636\(01\)00092-8](https://doi.org/10.1016/S0167-6636(01)00092-8)
- Maleki M, Bayat M (2012) Experimental evaluation of mechanical behavior of unsaturated silty sand under constant water content condition. *Eng Geol* 141–142:45–56. <https://doi.org/10.1016/j.enggeo.2012.04.014>
- Mitchell JM (1976) *Fundamental of soil behaviour*. Wiley, New Jersey
- Mohammadi A, Qadimi A (2015) A simple critical state approach to predicting the cyclic and monotonic response of sands with different fines contents using the equivalent intergranular void ratio. *Acta Geotech* 10:587–606. <https://doi.org/10.1007/s11440-014-0318-z>
- Mulilis JP, Arulanandan K, Mitchell JK, Chan CK, Seed HB (1977) Effects of sample preparation on sand liquefaction. *J Geotech Eng Div* 103:91–108
- Naemi SA, Baziar MH (2004) Effect of fines content on steady-state strength of mixed and layered samples of a sand. *Soil Dyn Earthq Eng* 24:181–187. <https://doi.org/10.1016/j.soildyn.2003.11.003>
- Ng CWW, Sadeghi H, Jafarzadeh F (2016) Compression and shear strength characteristics of compacted loess at high suctions. *Can Geotech J* 54:690–699. <https://doi.org/10.1139/cgj-2016-0347>
- Nguyen TK, Benahmed N, Hicher PY, Nicolas M (2015) The influence of fines content on the onset of instability and critical state line of silty sand. In: Chau K-T, Zhao J (eds) *Bifurcation and degradation of geomaterials in the new millennium*. Springer, Cham, pp 113–120
- Nishimura T, Fredlund DG (2002) Hysteresis effects resulting from drying and wetting under relatively dry conditions. In: *Third international conference on unsaturated soils*, Recife, Brazil, p 31
- Patil UD, Puppala AJ, Hoyos LR, Pedarla A (2017) Modeling critical-state shear strength behavior of compacted silty sand via suction-controlled triaxial testing. *Eng Geol* 231:21–33. <https://doi.org/10.1016/j.enggeo.2017.10.011>
- Pereira A, Feuerharmel C, Gehling W, Bica A (2006) A study on the shear strength envelope of an unsaturated colluvium soil. In: *Proceedings of the fourth international conference on unsaturated soils*, Arizona, USA, pp 1191–1199
- Pitman TD, Robertson PK, Sego DC (1994) Influence of fines on the collapse of loose sands. *Can Geotech J* 31:728–739. <https://doi.org/10.1139/t94-084>
- Polito CP (1999) The effects of non-plastic and plastic fines on the liquefaction of sandy soils. Dissertation, Virginia Tech
- Rahardjo H, Heng OB, Choon LE (2004) Shear strength of a compacted residual soil from consolidated drained and constant water content triaxial tests. *Can Geotech J* 41:421–436. <https://doi.org/10.1139/t03-093>
- Rahman MM, Lo SR (2007) On intergranular void ratio of loose sand with small amount of fines. In: *10th Australia New Zealand conference on geomechanics: common ground*. Brisbane, Australia, pp 674–679
- Rahman MM, Lo SR (2008) The prediction of equivalent granular steady state line of loose sand with fines. *Geomech Geoen* 3:179–190. <https://doi.org/10.1080/17486020802206867>
- Rahman MM, Cubrinovski MRLS, Lo SR (2012) Initial shear modulus of sandy soils and equivalent granular void ratio. *Geomech Geoen* 7:219–226. <https://doi.org/10.1080/17486025.2011.616935>
- Schnellmann R, Rahardjo H, Schneider HR (2013) Unsaturated shear strength of a silty sand. *Geomech Geoen* 162:88–96. <https://doi.org/10.1016/j.enggeo.2013.05.011>
- Schofield A, Wroth P (1968) *Critical state soil mechanics*. McGraw-Hill, London
- Thevanayagam S (1998) Effect of fines and confining stress on undrained shear strength of silty sands. *J Geotech Geoenviron Eng* 124:479–491. [https://doi.org/10.1061/\(ASCE\)1090-0241\(1998\)124:6\(479\)](https://doi.org/10.1061/(ASCE)1090-0241(1998)124:6(479))
- Thevanayagam S (2000) Liquefaction potential and undrained fragility of silty soils. In: *Proceedings of the 12th world conference earthquake engineering*, Wellington, New Zealand, p 8
- Thevanayagam S, Shenthian T, Mohan S, Liang J (2002) Undrained fragility of clean sands, silty sands, and sandy silts. *J Geotech Geoenviron Eng* 128:849–859. [https://doi.org/10.1061/\(ASCE\)1090-0241\(2002\)128:10\(849\)](https://doi.org/10.1061/(ASCE)1090-0241(2002)128:10(849))
- Toll D (1990) A framework for unsaturated soil behavior. *Géotechnique* 40:31–44. <https://doi.org/10.1680/geot.1990.40.1.31>
- Toll DG, Ong BH (2003) Critical-state parameters for an unsaturated residual sandy clay. *Géotechnique* 53:93–103. <https://doi.org/10.1680/geot.2003.53.1.93>
- Wang Q, Pufahl DE, Fredlund DG (2002) A study of critical state on an unsaturated silty soil. *Can Geotech J* 39:213–218. <https://doi.org/10.1139/t01-086>
- Wang Y, Tian H, Fan Y (2010) Effect of stress paths on shear strength response of unsaturated gassy sand from Hangzhou metro project. In: *Experimental and applied modeling of unsaturated soils*, Shanghai, China, pp 26–31
- Wheeler SJ, Sivakumar V (1995) An elasto-plastic critical state framework for unsaturated soil. *Géotechnique* 45:35–53. <https://doi.org/10.1680/geot.1995.45.1.35>
- Xenaki VC, Athanasopoulos GA (2003) Liquefaction resistance of sand–silt mixtures: an experimental investigation of the effect of fines. *Soil Dyn Earthq Eng* 23:1–12. [https://doi.org/10.1016/S0267-7261\(02\)00210-5](https://doi.org/10.1016/S0267-7261(02)00210-5)
- Yang S, Sandven R, Grande L (2006) Instability of sand–silt mixtures. *Soil Dyn Earthq Eng* 26:183–190. <https://doi.org/10.1016/j.soildyn.2004.11.027>

Zhou WH, Xu X, Garg A (2016) Measurement of unsaturated shear strength parameters of silty sand and its correlation with unconfined compressive strength. *Measurement* 93:351–358. <https://doi.org/10.1016/j.measurement.2016.07.049>

**Publisher's Note** Springer Nature remains neutral with regard to jurisdictional claims in published maps and institutional affiliations.